Bulletin of Engineering Geology and the Environment (2021) 80:2283–2305
https://doi.org/10.1007/s10064-020-02057-6

ORIGINAL PAPER

Optimized ANN model for predicting rock mass quality ahead of tunnel face using measure-while-drilling data

Jiankang Liu[1] · Yujing Jiang[1] · Wei Han[1] · Osamu Sakaguchi[1,2]

Received: 3 February 2020 / Accepted: 29 November 2020 / Published online: 7 January 2021

Abstract

Rock mass quality assessment has a vital influence on the excavation of tunnels and caverns in rock mass. For this purpose, extensive field studies, including records of measure-while-drilling data and rock mass quality scores (RQS) from the observation reports of tunnel faces, have been conducted. In order to predict RQS, three optimized artificial neural network (ANN) models based on genetic algorithm (GA), particle swarm optimization (PSO), and imperialist competition algorithm (ICA) were developed. Six parameters of measure-while-drilling (MWD) data and their corresponding RQS constituted 1270 datasets, which were set as input and output of ANN, respectively. The traditional multiple linear regression (MLR), multiple nonlinear regression (MNR) statistical model, and ANN model were developed as comparative models. Comparison results reveal that PSO-ANN and ICA-ANN models are capable of predicting RQS with higher reliability than the MLR, MNR, ANN, and GA-ANN models. Results indicate that PSO-ANN and ICA-ANN models can be used to predict RQS; however, the PSO-ANN model has better performance.

Keywords Rock mass quality score · Tunnel face · Artificial neural network · Hybrid model

Introduction

The assessment of rock mass quality is one of the main issues that affect the support design and operation cost of tunnel engineering (Lowson and Bieniawski 2013; Rehman et al. 2018). Inaccurate evaluation may cause the failure of support, and even lead to irreparable disasters such as water and mud gushing (Lu and Liu 2009; Li et al. 2017; Han et al. 2020) and sudden collapse of a tunnel (Shin et al. 1999). Accurate, effective, and objective rock mass quality assessment can reduce the cost and improve safety for tunnel engineering (Wang et al. 2020b).

In recent decades, the most commonly employed rock mass quality assessment system is the rock quality designation (RQD) system (Deere 1964), Norwegian geotechnical institute Q-system (Q) (Barton et al. 1974), rock mass rating (RMR) system (Bieniawski 1973), and geological strength index (GSI) system (Hoek and Brown 1997). In Japan, the Japan Highway Public Corporation (JH) system, which is based on the RMR system, is commonly used to quantitatively evaluate the rock mass quality (Masahiro et al. 1999; Akagi et al. 2001; Yuji et al. 2006). Similar to other assessment systems (e.g., Q-system, RMR system, and GSI system), when the JH system is utilized, the rock mass quality score (RQS), the scores of tunnel face observation items (e.g., compressive strength, weathering, and spacing of joints), is utilized to evaluate and grade the rock mass quality. Although these proposed assessment systems are extensively employed in rock engineering and tunnel engineering, the objectivity of the evaluation is insufficient due to subjective judgments that are based on the engineer's experience observation items (Palmstrom 2005; Rahmati et al. 2014; Zolfaghari et al. 2015; Wang et al. 2020a).

Over the last decades, with the development of measure-while-drilling (MWD) technology, this technology can be used to predict and evaluate rock mass quality in broad tunneling projects (Lear and Dareing 1990; Nilsen 2015; Navarro et al. 2018). Aoki et al. (1999) proposed to use MWD data to evaluate the geological conditions of different drilling depths.

✉ Yujing Jiang
jiang@nagasaki-u.ac.jp

[1] Graduate School of Engineering, Nagasaki University, 1-14 Bunkyo-machi, Nagasaki 852-8521, Japan

[2] Department of Civil Engineering, Konoike Construction Co., Ltd., 3-6-1, Kitakyuhoji-machi, Chuo-ku, Osaka 541-0057, Japan

Yue et al. (2004) used the MWD data to study decomposition grades in the ground, and confirmed that there is a certain relationship between the drilling speed and decomposition. Zhou et al. (2011) developed an unsupervised method to predict rock types based on MWD data, who verified that the method is effective in rock type recognition. Leung and Scheding (2015) adopted a modulation-specific energy to overcome the low specificity and high variability of existing MWD methods. Considering hundreds of thousands or more MWD data, the more efficient prediction method of fitting these MWD data to a rock mass quality index should be further developed.

With the development of artificial neural network (ANN) technology, the application of ANN in rock mass quality prediction has been successful (Sousa et al. 2012). Xu et al. (2007) used a back-propagation neural network to assess the rock mass quality. The RMR values were estimated by Hussain et al. (2016), who compared ANN technology with multiple regression technology. Karlaftis (2018) proposed an ANN model to classify rock masses using data from tunnels in Greece. The results demonstrated that the ANN can place a rock mass in the classification ratings very quickly and with very high accuracy with a smaller number of input variables. The applicability of ANN technology for an automatic online classification of rock mass was explored by Erharter et al. (2019). This research obtained a final classification accuracy of 74.4%.

ANN is one of the most innovative research fields in the field of science and engineering, with strong nonlinear mapping ability (Mohamad et al. 2012; Momeni et al. 2015). However, slow learning speed and easy to fall into local minima are some defects of ANN (Armaghani et al. 2018, 2019). Applications of population-based evolutionary algorithms, such as genetic algorithm (GA), particle swarm optimization (PSO), and imperialist competitive algorithm (ICA), are helpful to overcome these shortcomings. Using these algorithms to optimize artificial neural network can solve complex engineering problems and become a research hotspot (Hasanipanah et al. 2017; Khandelwal et al. 2017; Liu et al. 2020).

Although the feasibility of traditional rock mass quality assessment system has been identified, research on the development of more objective, intelligent, and efficient evaluation methods require further study. The purpose of this research is to introduce hybrid ANN technologies, including GA-ANN, PSO-ANN, and ICA-ANN, to predict the RQS (a rock mass quality index used in Japan) using the MWD data obtained from the new Nagasaki tunnel (east) of the West Kyushu line of the high-speed railway project in Japan. A conventional regression model and simple ANN model are developed. Subsequently, three hybrid ANNs are established and compared with the developed regression model and ANN model. Through comparative analysis, the best model to predict RQS value is selected. This method can evaluate rock mass quality accurately, effectively, and objectively.

Case study and dataset collection

Case study

A case study of the new Nagasaki tunnel in Japan was carried out. Excavation of the tunnel, which connects Nagasaki City and Isahaya City in southeastern Nagasaki province and central Nagasaki province, respectively, commenced in March 2013. As shown in Fig. 1, the MWD data of this study were obtained from the Nagasaki tunnel (east), with a length of 3.885 km, and adjacent to it is the new Nagasaki tunnel (west), with a length of 3.575 km. The New Austrian Tunneling Method was employed. The stratum exposed by this tunnel is mainly volcanic rock. The type of rock passing from west to east is propylite andesite, hornblende andesite,

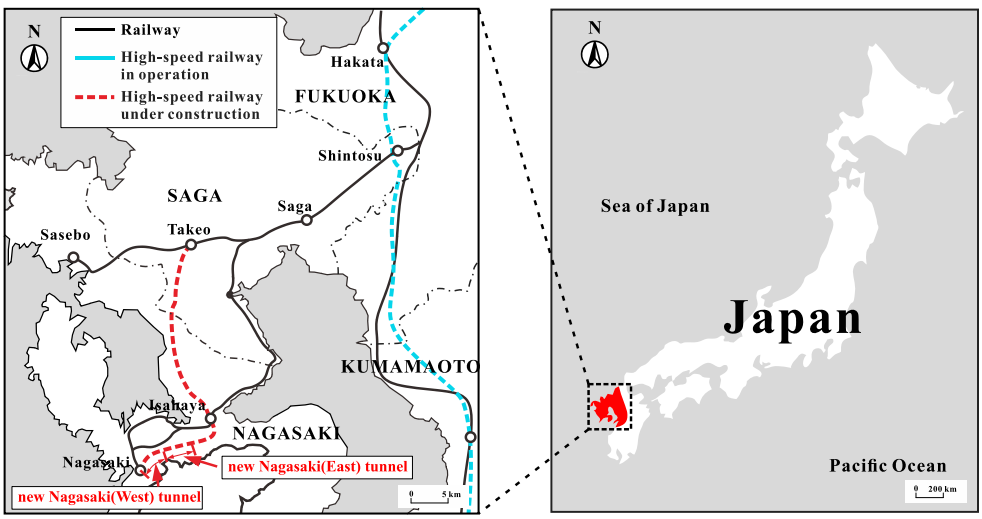

Fig. 1 Locations of the new Nagasaki tunnel (east) high-speed railway

tuff breccia, pyroxene andesite, and tuff breccia. Among them, propylite andesite accounts for the largest proportion, about 3 km. The geological condition of the surrounding rock is poor, and the measured compressional wave velocity (P wave) ranges from 2.5 to 3.5 km/s.

During tunnel excavation, the JH method based on the observation report of tunnel face was adopted to evaluate the rock mass exposed by the tunnel. This method uses ten rock parameters of total state, self-stability, intact rock strength, weathering, joint proportion, spacing of joints, joint aperture, distribution of joints, ground water inflow, and ground water deterioration to evaluate the rock mass quality. As shown in Table 1, when using the JH method for rock mass classification, all observation items are configured with four values from 1 to 4. The sum of each item value is the final rock rating score, which is called the RQS value. The larger RQS value represents the worse geological conditions of the tunnel and the higher support strength is required.

At the same time of tunnel excavation, the MWD data of drilling in advance working face were recorded. Figure 2 shows the drilling equipment and data collection equipment. The parameters of MWD data include the penetration rate (PR), hammer pressure (HP), rotation pressure (RP), feed pressure (FP), hammer frequency (HF), and specific energy (SE). The MWD data and the corresponding RQS constitute one dataset.

Dataset collection and analysis

In the process of tunneling, a total of 1270 datasets were collected in the new Nagasaki tunnel (east). To model and predict the RQS value, six parameters of MWD data were considered the input parameters. The RQS value was calculated form the observation report of the tunnel face. As shown in Table 2, descriptive statistics of parameters in the datasets were carried out. Their visual statistic distribution is provided in Fig. 3. The statistical results show that the values are extensively distributed. In addition, the correlation between each MWD parameter and their corresponding RQS was investigated. Figure 4 shows the distribution trend of each MWD parameter and RQS value along the tunnel chainage. The coefficient of determination (R^2) of each MWD parameter and the corresponding RQS were calculated, as shown in Fig. 5. As shown in Figs. 4 and 5, a positive correlation exists among RQS and PR, HP, HF, and FE, while a negative correlation exists for RP and FP. The correlation between RQS and FP is better than that of other parameters; however, a low correlation factor ($R^2 = 0.395$) is obtained. These results show a low correlation between MWD data and the RQS. The proportion of the R^2 value obtained by calculating each MWD parameter in the total R^2 value obtained by all parameters is taken as the

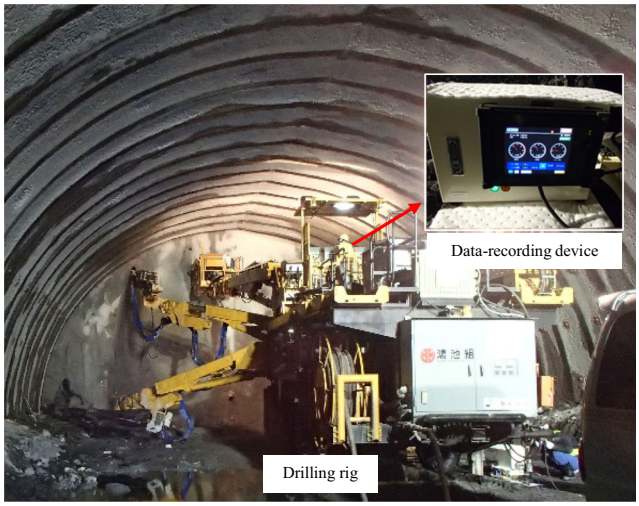

Fig. 2 Drilling rig and data-recording device

Table 1 Grading configuration of each item of rock masses

Item	Description	Evaluation score			
		1	2	3	4
1	Total state	Stable	Rock fall	Pressed	Collapse or outflow
2	Self-stability	Able	Gradual instability	Unable, primary support	Unable, pre-support
3	Intact rock strength, MPa	> 100	20–100	5–20	< 5
4	Weathering	Unweathered	Slightly weathered	Moderately weathered	Highly weathered
5	Joint proportion	< 5%	5–20%	20–50%	> 50%
6	Spacing of joints	> 1 m	0.2–1 m	50–200 mm	< 50 mm
7	Joint aperture	Highly closed	Moderately closed	Slightly closed	Unclosed
8	Morphology of joints	Random square	Columnar	Layered	Psammitic
9	Ground water inflow	None	Slight	Moderate	Heavy
10	Ground water deterioration	Uncorroded	Slightly deteriorated	Moderate deteriorated	Heavily deteriorated

Table 2 Distribution statistics of dataset parameters

Parameter	Description	Symbol	Mean	Min	Max	Std. dev
Input	Penetration rate	PR	1.00	0.08	4.44	0.62
	Hammer presser	HP	14.88	9.41	16.80	0.90
	Rotation pressure	RP	4.45	0.50	12.50	1.46
	Feed pressure	FP	3.87	0.90	8.70	1.31
	Hammer frequency	HF	32.14	0.00	60.00	13.70
	Specific energy	SE	285.49	34.90	3281.00	212.01
Output	Rock mass quality score	RQS	23.86	16.00	31.00	4.53

influence weight for each MWD parameter on the estimation of RQS. Through calculation, parameters PR, HP, RP, FP, HF, and SE respectively obtain weight values of 0.26, 0.01, 0.11, 0.36, 0.05, and 0.20. The results show that parameter FP has the greatest influence on the estimation of RQS, while parameter HP has the least. At the same time, a correlation analysis between input parameters was carried out. The correlation results of the parameters evaluated by power, exponential, and linear equations are shown in Fig. 6. Considering the evaluation index of R^2, the equation is evaluated. Figure 6 shows a high correlation between PR and SE; however, not too much R^2 value ($R^2 = 0.739$) is obtained. These results show that the correlation between the parameters is low. Therefore, using all of the MWD parameters to develop prediction model requires further study. The above analysis shows that the prediction ability of the model developed with a single MWD parameter is weak, and the modeling analysis of multiple MWD parameters needs to be carried out. In the following sections, the attempt to apply an advanced hybrid ANN technology to develop the RQS prediction models by multiple MWD parameters will be carried out.

To reduce the influence of the order of magnitude, the datasets were normalized by following equation:

$$X_{\text{norm}} = \frac{x - x_{\min}}{x_{\max} - x_{\min}} \quad (1)$$

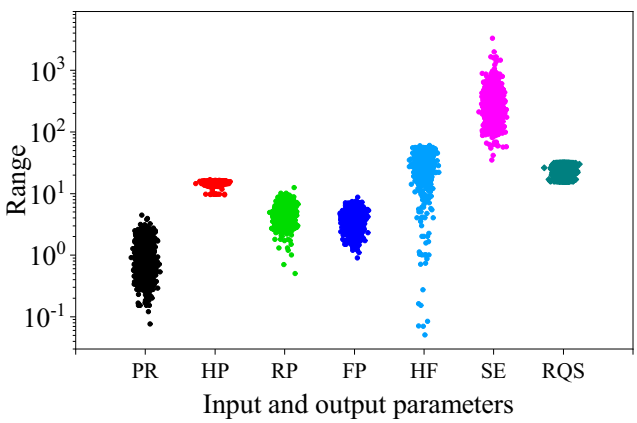

Fig. 3 Distribution of the parameters of the input data and output data

where X_{norm} and x are normalized data and measured data, respectively. $x_{\min}$ and $x_{\max}$ are the minimum value and maximum value, respectively, of x. The established datasets were divided into training set and testing set, to establish and evaluate the created networks. In order to train these datasets, Swingler (1996), Looney (1996), and Nelson and Illingworth (1991) proposed 80%, 75%, and 70–80% of the whole datasets as training sets respectively. In this study, the ratio of training set and testing set was set to 8:2, which means that there are 1016 datasets for training prediction models and 254 datasets for testing the predictability of the developed prediction model.

Methods

MLR and MNR

Multiple regression analysis is a statistical analysis method that considers one variable a dependent variable and at least two other variable independent variables to establish a linear or nonlinear mathematical relationship among multiple variables (Knofczynski and Mundfrom 2008). Multiple regression techniques are commonly used to predict the dependent variable by the independent variables. The multiple linear regression (MLR) equation is , $Y = b_1x_1 + b_2x_2 + \cdots + b_nx_n + c$ where b_i is a regression coefficient, x_i is the independent variable, Y is the dependent variable, and c is the intercept. The form of multiple nonlinear regression (MNR) equation is generally determined by the relationship between each independent variable and dependent variable.

ANN

ANN was invented by McCulloch and Pitts (McCulloch and Pitts 1943), who show that, in principle, ANNs can calculate any arithmetic or logic function. The work of these researchers is often regarded as the origin of the field of ANN. Rosenblatt (1958) invented a perceptron network and associated learning rules and demonstrated its ability of pattern recognition, which marked the first practical application of ANN. The successful

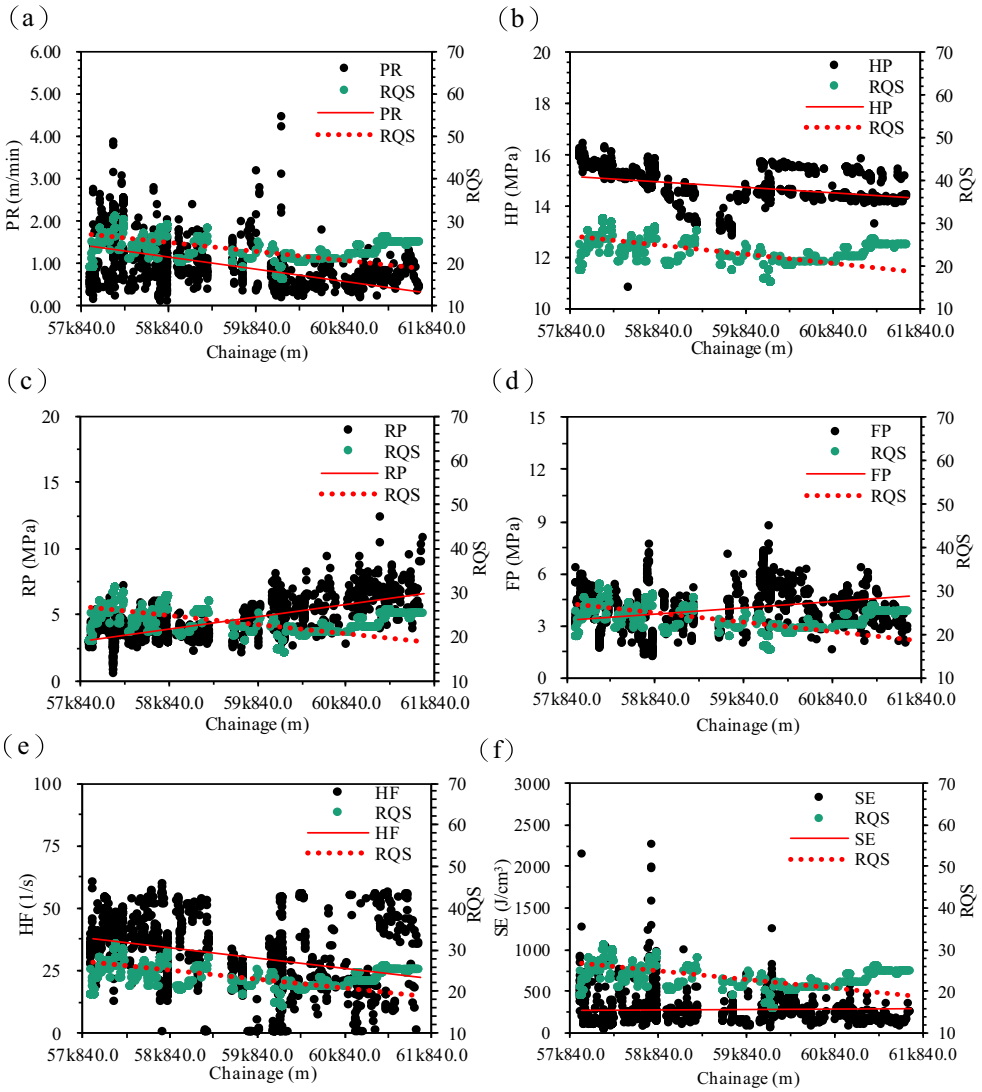

Fig. 4 Distribution trend of among RQS and MWD parameters. **a** PR. **b** HP. **c** RP. **d** FP. **e** HF. **f** FE

application of a neural network generated substantial interest in the research of the ANN. However, subsequent research showed that the performance of the basic perceptron network was limited. ANNs became a research hotspot in the late 1980s as information processing structures that were inspired by a biological neural organization structure and operation mode. An ANN is a system composed of several nodes (neurons). These basic nodes are connected and work in parallel to complete certain processing tasks. ANNs can automatically derive general rules by provided pairs of input and output signals. Using this rule, an ANN can generate prediction output for previously unused signals.

The traditional nonlinear regression technique is a highly fitting method for general nonlinear functions, which is based on the nonlinear structure of each element that is linearly combined. As a "universal approximation" technology, ANN is proved to be an " Input-Hidden-Output " hierarchical structure, which enables it to fit almost all functions (including nonlinear functions) (Hornik 1991; Back and Chen 2002; Monjezi et al. 2013). The nonlinear fitting ability of ANN is mainly attributed to the ability to express the properties of each element and the organizational structure between elements. In this research, a typical three-layer neural network is adopted to developed ANN models (Fig. 7). Figure 7 also shows the processing flow of ANN, including training stage and testing stage. In the training stage, the input and output of training dataset are input to the input layer of ANN in pairs. Then, the relationship between the training datasets was established by one training algorithm. The remainder of the dataset was applied as a testing dataset. The error back-propagation algorithm is employed as the training algorithm. This algorithm includes two passes: feed-forward pass and backward propagation pass. In the feed-forward pass, the output value of network and the weight and biases of network nodes are random. In the process of the backward propagation pass, the actual values of the outputs are subtracted from the calculated values in a previous pass to generate an error signal. The signal propagates backward to the input layer. According

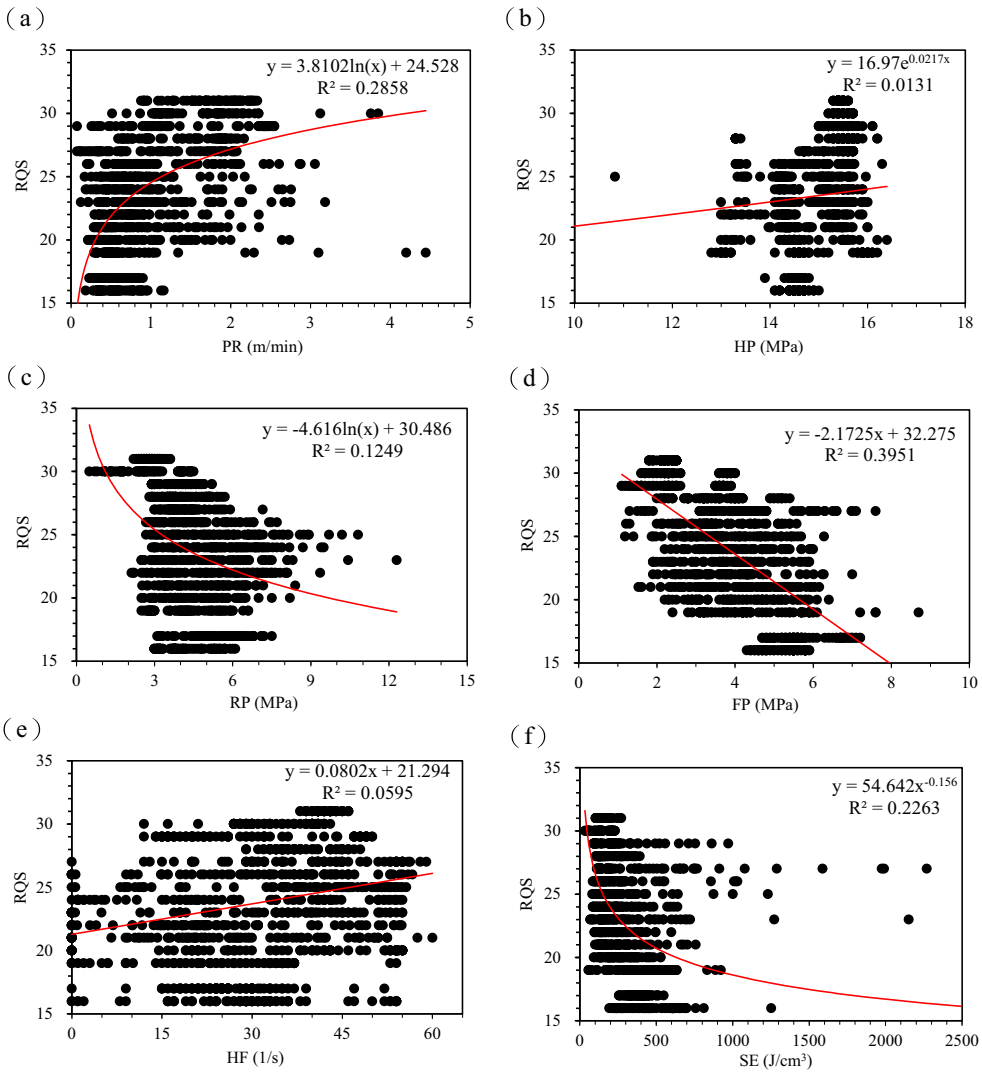

Fig. 5 The correlation among RQS and MWD parameters. **a** PR. **b** HP. **c** RP. **d** FP. **e** HF. **f** FE

to this signal, the weight and biases are adjusted until the set condition is reached.

GA

The GA was developed by Holland (1992) to find the optimal solution based on the theory of natural evolution. The genetic operation of a GA consists of selection, crossover, and mutation. The GA has many advantages, such as no limit of derivation and function continuity, and better global optimization ability. Despite the advantages of the GA, it has numerous problems. These problems include difficult operator parameter selection, slow search speed, and dependence on initial population selection. However, GAs continue to be extensively employed in approximating nonlinear optimization (Yang 2010). In the first stage of the general process of GA, the problem solutions are encoded (e.g., binary encoding or real encoding). In the second stage, the loop process is executed by randomly generating chromosomes. In the final stage, the fitness of each chromosome is calculated. Two individuals are selected from the population for crossover and mutation based on the fitness and selection probability. A crossover operator is used to randomly select two chromosomes of the selected individuals to produce the next generation. A mutation operator is utilized to randomly select the chromosomes of the new generations for the mutation operation. The cycle is repeated until the stop condition is satisfied (Dybowski et al. 1996; Nasseri et al. 2008).

PSO

PSO, which is also a heuristic algorithm, is an evolutionary computing technology that was proposed by Kennedy and Eberhart (1995). Particle position and velocity are the core operators of PSO. The motion of particle is the process of individual search. The movement velocity of each particle is adjusted according to the historical optimal position of all particles and the historical optimal position of each particle. The optimal solution that each particle individually searches is referred to

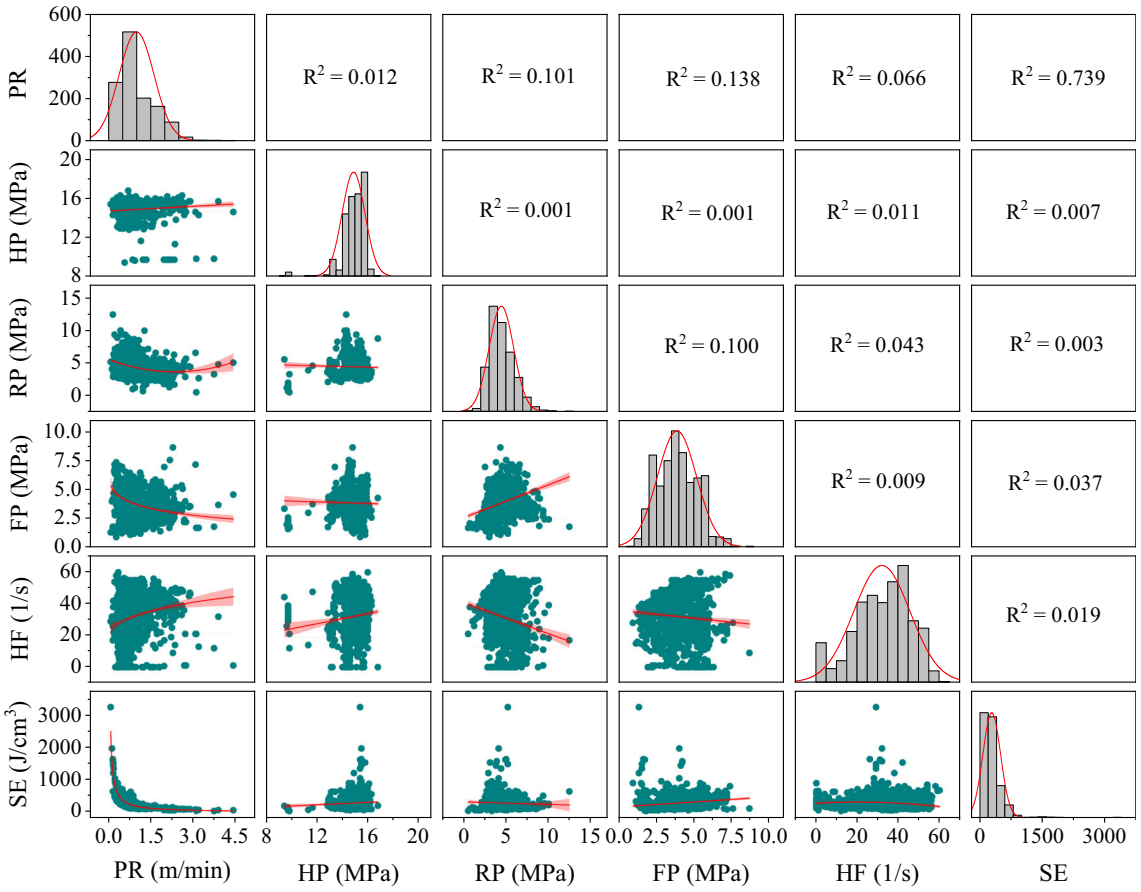

Fig. 6 Correlation analysis among the input parameters

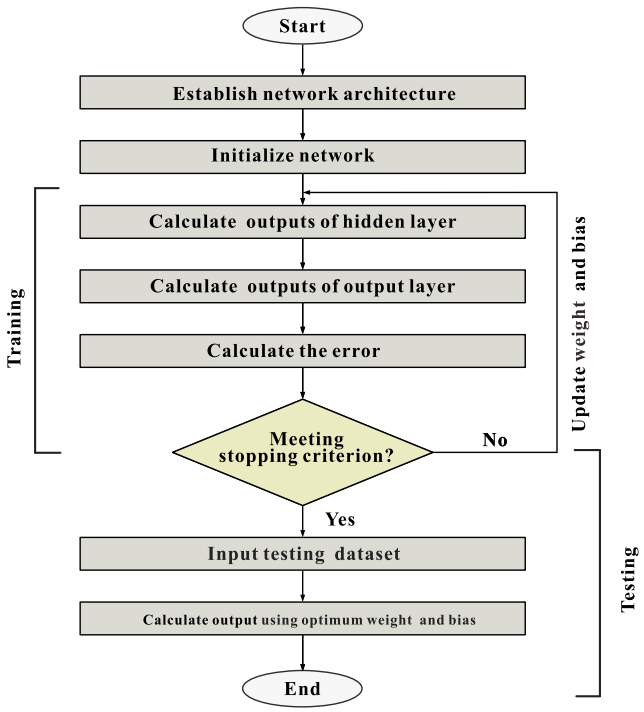

Fig. 7 Flowchart of the artificial neural network

as the personal best (p_{best}), and the optimal individual extremum of all particles is the current global best (g_{best}). The velocity and particle position were updated (Eqs. (2) and (3)). The optimal solution is obtained by cyclic iteration.

$$v_{new} = wv + c_1 r_1 (p_{best} - p) + c_2 r_2 (g_{best} - p) \quad (2)$$

$$p_{new} = p + v_{new} \quad (3)$$

where v_{new}, v, p_{new}, p, and w are the new velocity, current velocity, new position, current position, inertia weight, respectively. r_1 and r_2 are random numbers that are usually chosen between [0, 1]. c_1 is a positive constant, which is referred to as the coefficient of self-adjustment, and c_2 is a positive constant, which is referred to as the coefficient of the social component. p_{best} and g_{best} are the best locations for individuals and the best locations for all particles. PSO has been widely used in civil engineering, traffic engineering, and other engineering fields. A detailed description of PSO and its application in different subjects are provided in the literature (Shi and Eberhart 1998; Gandomi et al. 2013; Nouiri et al. 2018).

ICA

Inspired by the colonial competition mechanism of imperialism, Atashpaz-Gargari and Lucas (2007) proposed a new

Table 3 The performance index results of different number of hidden nodes for predicting RQS

Model no.	Nodes in hidden layer	Index	Result											Average result	Rank value		Total
			Run 1		Run 2		Run 3		Run 4		Run 5						
			Training	Testing	Training	Testing	Training	Testing	Training	Testing	Training	Testing	Training	Testing	Training	Testing	
1	1	R^2	0.543	0.624	0.543	0.616	0.542	0.622	0.542	0.623	0.543	0.620	0.542	0.618	1	1	2
2	2		0.652	0.680	0.639	0.656	0.540	0.611	0.658	0.657	0.627	0.664	0.621	0.652	2	2	4
3	3		0.700	0.700	0.726	0.727	0.720	0.769	0.663	0.712	0.548	0.626	0.663	0.706	3	5	8
4	4		0.690	0.567	0.783	0.803	0.712	0.715	0.622	0.690	0.786	0.796	0.724	0.752	4	8	12
5	5		0.735	0.744	0.758	0.784	0.773	0.775	0.807	0.826	0.761	0.749	0.767	0.777	10	20	30
6	6		0.740	0.762	0.664	0.675	0.788	0.795	0.803	0.834	0.740	0.702	0.759	0.760	5	17	22
7	7		0.753	0.779	0.777	0.802	0.661	0.670	0.820	0.822	0.798	0.804	0.759	0.761	7	22	29
8	8		0.828	0.804	0.748	0.738	0.686	0.707	0.824	0.837	0.733	0.722	0.760	0.765	8	18	26
9	9		0.822	0.835	0.701	0.623	0.810	0.804	0.722	0.701	0.806	0.748	0.770	0.736	11	14	25
10	10		0.786	0.756	0.810	0.824	0.843	0.824	0.790	0.799	0.775	0.751	0.796	0.794	18	23	41
11	11		0.677	0.668	0.843	0.823	0.682	0.694	0.813	0.781	0.751	0.686	0.771	0.733	6	11	17
12	12		0.759	0.693	0.840	0.838	0.830	0.826	0.802	0.814	0.815	0.783	0.815	0.806	20	24	44
13	13		0.797	0.780	0.812	0.781	0.834	0.814	0.872	0.846	0.754	0.657	0.825	0.784	21	21	42
14	14		0.733	0.710	0.840	0.734	0.728	0.670	0.770	0.745	0.792	0.770	0.790	0.749	12	10	22
15	15		0.835	0.825	0.835	0.840	0.825	0.786	0.829	0.758	0.836	0.833	0.833	0.803	25	26	51
16	16		0.784	0.732	0.814	0.724	0.804	0.783	0.853	0.835	0.833	0.765	0.819	0.782	24	19	43
17	17		0.691	0.660	0.770	0.721	0.836	0.838	0.758	0.698	0.836	0.769	0.807	0.762	13	13	26
18	18		0.860	0.815	0.793	0.789	0.807	0.649	0.676	0.704	0.753	0.708	0.766	0.729	14	12	26
19	19		0.834	0.814	0.844	0.813	0.670	0.682	0.745	0.731	0.730	0.701	0.727	0.718	9	16	25
20	20		0.875	0.544	0.767	0.493	0.851	0.828	0.774	0.756	0.811	0.801	0.788	0.707	23	3	26
21	30		0.751	0.678	0.797	0.789	0.860	0.770	0.730	0.669	0.765	0.632	0.802	0.739	15	6	21
22	40		0.782	0.719	0.813	0.757	0.783	0.623	0.783	0.689	0.791	0.702	0.803	0.714	17	4	21
23	50		0.828	0.809	0.855	0.605	0.795	0.718	0.714	0.672	0.837	0.792	0.810	0.720	19	9	28
24	60		0.842	0.824	0.871	0.814	0.761	0.675	0.777	0.649	0.819	0.757	0.797	0.700	22	15	37
25	70		0.843	0.799	0.821	0.757	0.867	0.762	0.821	0.803	0.886	0.840	0.832	0.769	26	25	51
26	80		0.782	0.672	0.771	0.726	0.838	0.777	0.798	0.699	0.750	0.666	0.811	0.702	16	7	23
1	1	RMSE	3.023	2.948	3.024	2.988	3.026	2.959	3.025	2.962	3.023	2.965	3.026	2.978	1	1	2
2	2		2.640	2.704	2.690	2.813	3.034	2.992	2.617	2.802	2.740	2.751	2.752	2.816	2	3	5
3	3		2.452	2.618	2.342	2.484	2.365	2.292	2.596	2.564	3.008	2.938	2.584	2.593	3	7	10
4	4		2.488	3.222	2.085	2.111	2.403	2.549	2.751	2.672	2.073	2.155	2.340	2.366	4	9	13
5	5		2.302	2.435	2.200	2.204	2.130	2.251	1.964	1.986	2.189	2.365	2.157	2.233	9	21	30
6	6		2.282	2.335	2.591	2.718	2.057	2.152	1.985	1.930	2.281	2.629	2.182	2.316	5	17	22

Table 3 (continued)

Model no.	Nodes in hidden layer	Index	Result											Average result	Rank value		Total
			Run 1		Run 2		Run 3		Run 4		Run 5						
			Training	Testing	Training	Testing	Training	Testing	Training	Testing	Training	Testing	Training	Testing	Training	Testing	
7	7		2.225	2.254	2.112	2.120	2.603	2.729	1.895	2.007	2.016	2.135	2.180	2.313	7	20	27
8	8		1.855	2.100	2.255	2.470	2.506	2.567	1.879	1.923	2.311	2.514	2.181	2.297	8	18	26
9	9		1.890	1.957	2.445	2.947	1.950	2.095	2.359	2.620	1.970	2.409	2.136	2.438	12	14	26
10	10		2.090	2.413	1.950	2.000	1.771	1.979	2.051	2.148	2.121	2.364	2.016	2.152	18	24	42
11	11		2.550	2.728	1.773	2.009	2.530	2.670	1.936	2.213	2.232	2.672	2.128	2.452	6	12	18
12	12		2.196	2.651	1.790	1.914	1.845	1.988	2.001	2.095	1.925	2.218	1.927	2.099	20	25	45
13	13		2.014	2.237	1.944	2.245	1.822	2.049	1.598	1.867	2.219	2.828	1.862	2.203	22	22	44
14	14		2.314	2.562	1.789	2.528	2.334	2.734	2.145	2.429	2.042	2.319	2.041	2.397	11	10	21
15	15		1.817	1.997	1.819	1.888	1.881	2.232	1.850	2.341	1.814	1.945	1.828	2.110	25	26	51
16	16		2.087	2.466	1.942	2.584	2.003	2.220	1.714	1.938	1.825	2.324	1.910	2.233	23	19	42
17	17		2.504	2.793	2.145	2.510	1.816	1.941	2.205	2.613	1.814	2.306	1.957	2.324	13	13	26
18	18		1.677	2.077	2.033	2.177	1.967	3.004	2.561	2.574	2.223	2.572	2.160	2.494	14	11	25
19	19		1.830	2.035	1.770	2.070	2.569	2.687	2.259	2.471	2.324	2.600	2.325	2.515	10	16	26
20	20		1.579	3.808	2.162	3.833	1.730	1.977	2.126	2.369	1.943	2.124	2.052	2.626	24	2	26
21	30		2.232	2.710	2.025	2.221	1.675	2.320	2.324	2.743	2.167	2.955	1.976	2.436	15	5	20
22	40		2.090	2.516	1.933	2.391	2.083	3.022	2.095	2.704	2.043	2.609	1.983	2.573	17	4	21
23	50		1.900	2.092	1.726	3.270	2.023	2.533	2.393	2.713	1.804	2.184	1.940	2.550	19	8	27
24	60		1.787	1.984	1.608	2.059	2.187	2.738	2.110	2.874	1.915	2.333	2.006	2.608	21	15	36
25	70		1.774	2.137	1.894	2.352	1.640	2.418	1.892	2.112	1.518	1.930	1.824	2.299	26	23	49
26	80		2.090	2.761	2.157	2.532	1.802	2.249	2.013	2.649	2.238	2.756	1.926	2.680	16	6	22

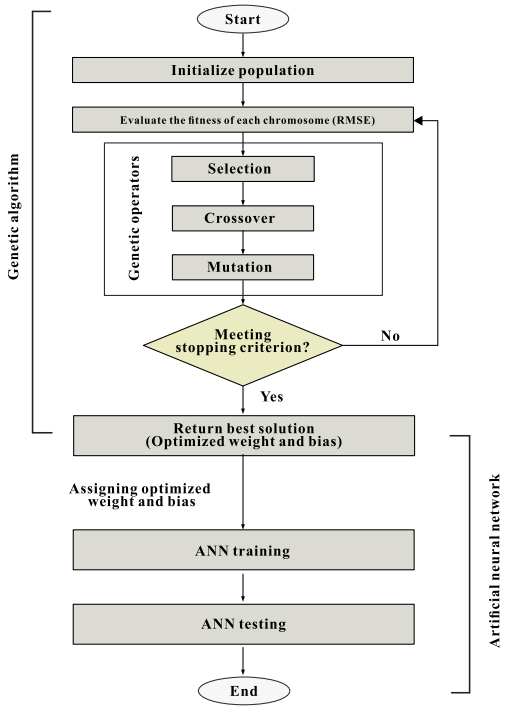

Fig. 8 Flowchart of the optimized artificial neural network by the genetic algorithm

intelligent optimization algorithm, imperialist competitive algorithm (ICA), in 2007. Different from GA, PSO, and other swarm intelligence algorithms inspired by biological behavior, ICA is an optimization method inspired by social behavior. ICA is also a population-based optimization algorithm. ICA divided the country into several empires. Within each empire, ICA brought the colonies closer to the imperialist countries through assimilation mechanism. Empire competition mechanism is an important operator of ICA algorithm. One or more weakest empires are annexed by the strongest empires through empire competition mechanism. Through the annexation of the empire, the exchange of information between the empires is completed. A more detailed description of the ICA and its application in different subjects is provided in the literature (Gazafroudi et al. 2014; Moayedi and Jahed Armaghani 2018).

Predictive models

MLR and MNR models

MLR and MNR prediction models were developed to correlate the RQS by the input parameters of PR, HP, RP, FP, HF, and SE of the training datasets. Equations (4) and (5) show the developed MLR and MNR model, respectively. The evaluations of these two models with testing datasets will be carried out in the "Results and discussion" section.

$$\begin{aligned} \mathrm{RQS} = {} & 13.082 + 1.845\mathrm{PR} \\ & + 1.034\mathrm{HP} - 0.142\mathrm{RP} - 1.717\mathrm{FP} \\ & + 0.032\mathrm{HF} - 0.001\mathrm{SE} \end{aligned} \tag{4}$$

Table 4 RQS prediction performance index results of the GA-ANN for different population size

No.	Population size	GA-ANN				Rank value				Total
		Training		Testing		Training		Testing		
		R^2	RMSE	R^2	RMSE	R^2	RMSE	R^2	RMSE	
1	25	0.801	1.975	0.786	2.191	3	3	4	6	16
2	50	0.840	1.787	0.792	2.179	12	12	10	10	44
3	75	0.800	1.991	0.771	2.259	2	2	1	1	6
4	100	0.844	1.765	0.791	2.186	14	14	9	9	46
5	150	0.822	1.882	0.787	2.196	8	7	6	5	26
6	200	0.813	1.924	0.782	2.243	5	5	3	2	15
7	250	0.837	1.804	0.808	2.083	11	11	13	13	48
8	300	0.844	1.770	0.818	2.036	13	13	14	14	54
9	350	0.831	1.825	0.788	2.230	10	10	7	3	30
10	400	0.822	1.879	0.807	2.086	7	8	12	12	39
11	450	0.805	1.970	0.787	2.188	4	4	5	7	20
12	500	0.797	2.003	0.781	2.212	1	1	2	4	8
13	550	0.816	1.913	0.789	2.187	6	6	8	8	28
14	600	0.823	1.859	0.800	2.130	9	9	11	11	40

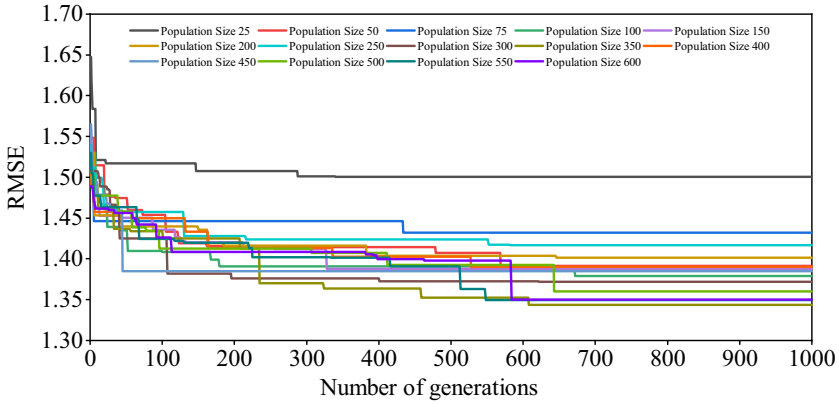

Fig. 9 Performance comparison of the GA-ANN models with the different number of generations

$$\mathrm{RQS} = 112.553 - 0.983\, ln(\mathrm{PR}) + 0.004e^{0.471\mathrm{HP}} - 2.165ln(RP) - 1.514\mathrm{FP} + 0.030\mathrm{HF} - 69.971\mathrm{SE}^{0.037} \quad (5)$$

In this study, the coefficient of determination (R^2), root mean square error (RMSE), and variance account for (VAF) indices were calculated to evaluate the prediction capacity of the developed models, as adopted by Yilmaz (2009) and Kayabasi (2012):

$$R^2 = 1 - \frac{\sum_{i=1}^{n} (y - y')^2}{\sum_{i=1}^{n} \left(y - \bar{y}\right)^2} \quad (6)$$

$$\mathrm{RMSE} = \sqrt{\frac{1}{n} \sum_{i=1}^{n} (y - y')^2} \quad (7)$$

$$\mathrm{VAF} = \left[1 - \frac{\mathrm{var}(y - y')}{\mathrm{var}(y)}\right] \quad (8)$$

where y is the ith measured value, y' is the ith predicted value, $\bar{y}$ is mean value of the y, and n is the number of datasets. High R^2 and VAF values and low RMSE values indicate that the prediction performance is superior. If the R^2 is 1, the RMSE is 0, and the VAF is 100, the model performance will be excellent.

ANN models

The prediction ANN model was proposed in this section. As previously mentioned, the Levenberg-Marquardt was employed as a training algorithm. Difficulty in establishing ANN model is encountered in selecting the number of hidden layer and nodes.

Many researchers reported that one hidden layer is usually enough to solve most problems. Therefore, the number of hidden layers in this study was set to one. The number of input and output layer nodes was set to 6 and 1, respectively. The prediction performance of ANN is mainly affected by the number of hidden nodes (Kanellopoulos and Wilkinson 1997; Gao 1998; Monjezi et al. 2011) to evaluate the influence of the number of hidden layer nodes on the performance of the ANN model. As shown in Table 3, 26 single hidden layer neural network models and 1–80 hidden layer nodes were constructed. Index R^2 and RMSE were used to evaluate the prediction performance of the developed models. However, it is difficult to determine the optimal model. Zorlu et al. (2008) proposed a simple sorting selection method to deal with the above difficulties in selecting the optimal model. The principle of this ranking method is that the highest score means the best performance. For example, R^2 values of 0.542, 0.621, 0.663, 0.724, 0.767, 0.759, 0.759, 0.760, 0.770, 0.796, 0.771, 0.815, 0.825, 0.790, 0.833, 0.819, 0.807, 0.766,

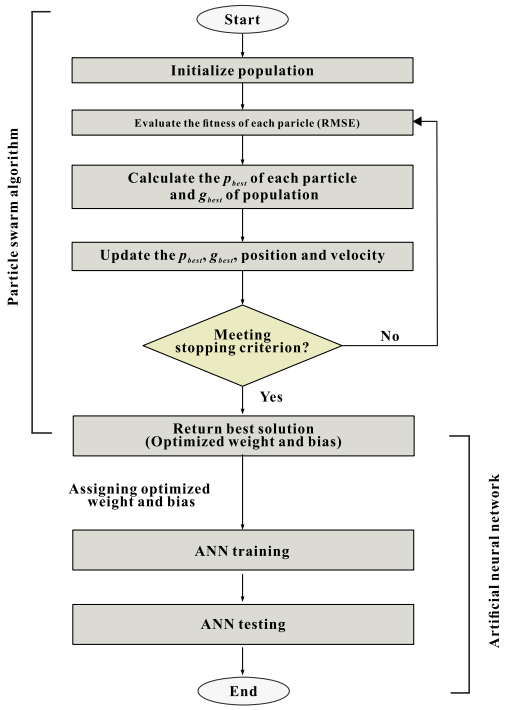

Fig. 10 Flowchart of the particle swarm optimization algorithm

Table 5 Effect of the swarm size on the hybrid PSO-ANN in predicting RQS

No.	Swarm size	PSO-ANN				Rank value				Total
		Training		Testing		Training		Testing		
		R^2	RMSE	R^2	RMSE	R^2	RMSE	R^2	RMSE	
1	25	0.821	1.878	0.782	2.238	6	7	5	5	23
2	50	0.807	1.952	0.760	2.331	1	1	1	1	4
3	75	0.833	1.822	0.805	2.105	11	10	10	10	41
4	100	0.839	1.793	0.777	2.313	13	13	4	2	32
5	150	0.824	1.878	0.776	2.274	8	8	3	3	22
6	200	0.819	1.899	0.795	2.169	4	4	7	7	22
7	250	0.809	1.943	0.792	2.172	2	2	6	6	16
8	300	0.832	1.820	0.817	2.041	9	12	12	12	45
9	350	0.845	1.751	0.802	2.113	14	14	8	8	44
10	400	0.833	1.822	0.812	2.068	10	11	11	11	43
11	450	0.834	1.824	0.820	2.017	12	9	14	14	49
12	500	0.821	1.884	0.803	2.112	7	6	9	9	31
13	550	0.820	1.891	0.775	2.261	5	5	2	4	16
14	600	0.819	1.906	0.817	2.018	3	3	13	13	32

0.727, 0.788, 0.802, 0.803, 0.810, 0.797, 0.832, and 0.811 were obtained for the training datasets of models 1–26, as shown in Table 3. The ratings of the models were assigned 1, 2, 3, 4, 10, 5, 7, 8, 11, 18, 6, 20, 21, 12, 25, 24, 13, 14, 9, 23, 15, 17, 19, 22, 26, and 16, respectively. This method was also used to evaluate RMSE results. Table 3 showed the final sorting results. Results revealed that the network model no. 15, which had one hidden layer with the neural network architecture of 6-15-1, was considered the optimum model for RQS prediction. According to the results in this table, model no. 15 representing the network structure of 6-15-1 was selected as the best prediction mode. Additional discussions regarding the optimum developed model (among 5 runs) is given in the "Results and discussion" section. It is noted that different hybrid models of the neural network structure were developed based on 6-15-1.

GA-ANN models

In this section, the hybrid model GA-ANN was established. Figure 8 shows the flowchart. The establishment process of hybrid GA-ANN prediction model for RQS is detailed in the following section.

GA parameters

The main parameters of GA are population size (S_{pop}), number of generations ($N_{gen\text{-}GA}$), mutation probability, and crossover probability. The main task of developing hybrid GA-ANN model is to determine these parameters. The mutation probability proposed by Momeni et al. (2014) was set to 25%, and the crossover probability was set to 70%. The roulette method was used as the selection method of crossover operation.

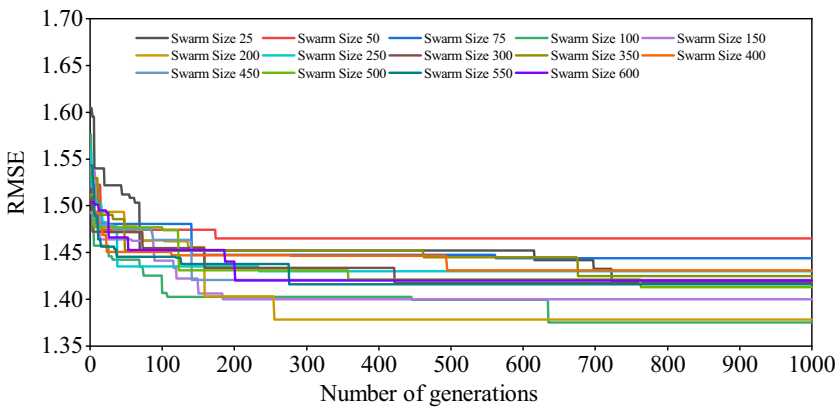

Fig. 11 Performance comparison of the PSO-ANN models with the different number of generations

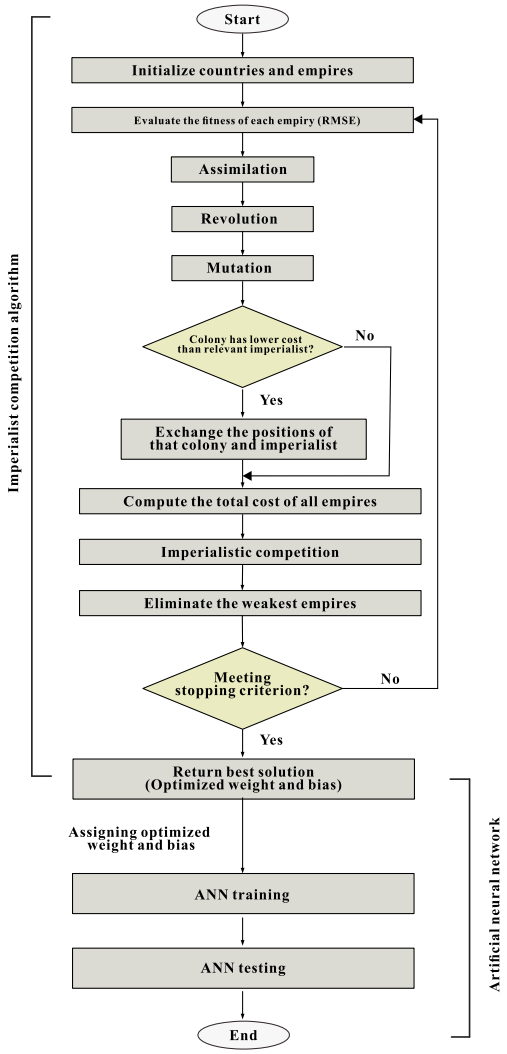

Fig. 12 Flowchart of the imperialist competitive algorithm

Value of the S_{pop}

Different GA-ANN models with population sizes between 25 and 600 were established to determine the best S_{pop} value, as shown in Table 4. It should be noted that these models were all developed with 6-15-1 neural network structure with the maximum generation of 100. Similar to the "ANN" model section, the simple sorting method was used to filter out the best S_{pop}. The results show that the model no. 8 has the optimal prediction performance. As a result, the best S_{pop} value was selected as 300.

Value of the $N_{gen\text{-}GA}$

A number of GA-ANN models were established to determine the most appropriate $N_{gen\text{-}GA}$ with the maximum number of 1000 and S_{pop} values of 25–600. Other parameters of GA-ANN used in these models were set as the parameters determined in the previous steps. As shown in Fig. 9, after 700 generations, the RMSE value no longer continues to decline and remains constant. Thus, a value of 700 was chosen as the optimum $N_{gen\text{-}GA}$.

Network modeling

Using the best parameters obtained in the above steps, the final hybrid GA-ANN model was established, and 5 times of training were carried out. The performance index values obtained of the development models are shown in Table 8. Further comparative analysis will be performed in the "Results and discussion" section.

Table 6 RQS prediction performance index results of the hybrid ICA-ANN for the different number of countries

No.	No. of country	ICA-ANN				Rank value				Total
		Training		Testing		Training		Testing		
		R^2	RMSE	R^2	RMSE	R^2	RMSE	R^2	RMSE	
1	50	0.816	1.913	0.801	2.114	5	5	7	8	25
2	75	0.836	1.801	0.778	2.255	9	10	2	2	23
3	100	0.794	2.019	0.784	2.190	1	2	4	3	10
4	150	0.826	1.867	0.816	2.025	6	6	10	13	35
5	200	0.831	1.833	0.802	2.120	7	7	8	7	29
6	250	0.859	1.667	0.813	2.049	13	13	9	10	45
7	300	0.805	1.967	0.784	2.185	3	3	3	4	13
8	350	0.831	1.819	0.817	2.028	8	8	13	12	41
9	400	0.796	2.020	0.791	2.175	2	1	5	5	13
10	450	0.844	1.758	0.816	2.042	12	12	12	11	47
11	500	0.837	1.809	0.816	2.050	10	9	11	9	39
12	550	0.813	1.929	0.768	2.295	4	4	1	1	10
13	600	0.840	1.786	0.794	2.173	11	11	6	6	34

Table 7 RQS prediction performance index results of the hybrid ICA-ANN for the different number of imperialists

No.	No. of imperialist	ICA-ANN				Rank value				Total
		Training		Testing		Training		Testing		
		R^2	RMSE	R^2	RMSE	R^2	RMSE	R^2	RMSE	
1	50	0.818	1.919	0.785	2.196	4	4	1	1	10
2	60	0.833	1.809	0.802	2.146	11	11	10	6	38
3	70	0.820	1.895	0.810	2.068	5	5	14	14	38
4	80	0.833	1.820	0.802	2.100	10	10	11	12	43
5	90	0.854	1.704	0.834	1.940	16	16	16	16	64
6	100	0.796	2.011	0.797	2.147	1	1	4	5	11
7	110	0.824	1.879	0.808	2.075	6	6	13	13	38
8	120	0.853	1.714	0.820	2.041	15	15	15	15	60
9	130	0.852	1.718	0.797	2.182	14	14	5	2	35
10	140	0.830	1.830	0.799	2.126	8	9	7	9	33
11	150	0.836	1.805	0.803	2.116	12	12	12	10	46
12	160	0.840	1.783	0.795	2.156	13	13	3	4	33
13	170	0.814	1.932	0.790	2.179	2	2	2	3	9
14	180	0.825	1.864	0.801	2.114	7	7	9	11	34
15	190	0.832	1.836	0.799	2.141	9	8	8	7	32
16	200	0.814	1.921	0.798	2.130	3	3	6	8	20

PSO-ANN models

Similar to the GA, several researchers have successfully employed the PSO to optimize ANN (Hoballah and Erlich 2009; Vasumathi and Moorthi 2012; Moayedi et al. 2019). In this section, the optimal parameters of the hybrid PSO-ANN model will be determined. Figure 10 shows the flowchart of the hybrid PSO-ANN algorithm.

PSO parameters

For PSO algorithm, the main parameters are the coefficient of velocity equation, number of particles (N_{par}), number of generations ($N_{par\text{-}PSO}$), c_1, c_2, and w. It should be emphasized that in the establishment of all PSO-ANN models, the values of c_1, c_2, and w were all set to $c_1 = c_2 = 2$ and w 0.25 recommended by Kennedy and Eberhart (1997) and Clerc and Kennedy (2002).

Value of the N_{par}

Several PSO-ANN models were established with a range of N_{par} from 25 to 600 to select the optimal N_{par} value, as presented in Table 5. The architecture of 6-15-1 and maximum generation of 100 were utilized, and the performance indices of R^2 and RMSE

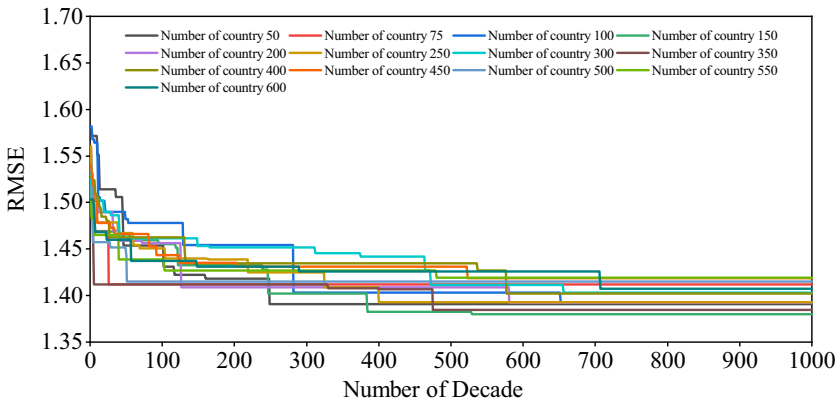

Fig. 13 Performance comparison of the ICA-ANN models with the different numbers of decades

Table 8 RQS prediction performance index results of the MLR, ANN, GA-ANN, PSO-ANN, and ICA-ANN models

Method	Stage	Model no.	R^2	RMSE	VAF	Rank value			Total
						R^2	RMSE	VAF	
MLR	Training	1	0.543	3.024	0.543	1	1	1	1
	Testing	1	0.621	2.964	0.615	1	1	1	1
MNR	Training	1	0.583	2.889	0.583	1	1	1	1
	Testing	1	0.659	2.800	0.654	1	1	1	1
ANN	Training	1	0.835	1.817	0.835	3	4	4	11
		2	0.835	1.819	0.835	4	3	3	10
		3	0.825	1.881	0.825	1	1	1	3
		4	0.829	1.850	0.829	2	2	2	6
		5	0.836	1.814	0.835	5	5	5	15
	Testing	1	0.825	1.997	0.824	3	3	3	9
		2	0.840	1.888	0.840	5	5	5	15
		3	0.786	2.232	0.779	2	2	2	6
		4	0.758	2.341	0.755	1	1	1	3
		5	0.833	1.945	0.833	4	4	4	12
GA-ANN	Training	1	0.830	1.863	0.828	3	3	3	9
		2	0.839	1.792	0.839	5	5	5	15
		3	0.833	1.828	0.833	4	4	4	12
		4	0.827	1.864	0.826	2	2	2	6
		5	0.820	1.899	0.820	1	1	1	3
	Testing	1	0.828	1.960	0.827	3	3	2	8
		2	0.816	2.038	0.814	1	1	1	3
		3	0.840	1.905	0.839	5	5	5	15
		4	0.827	1.980	0.827	2	2	3	7
		5	0.833	1.932	0.833	4	4	4	12
PSO-ANN	Training	1	0.836	1.815	0.835	2	2	3	9
		2	0.875	1.584	0.875	5	5	5	12
		3	0.868	1.629	0.867	4	4	4	15
		4	0.830	1.843	0.830	1	1	2	3
		5	0.866	1.638	0.829	3	3	1	6
	Testing	1	0.846	1.871	0.829	1	1	1	3
		2	0.862	1.782	0.861	5	5	5	9
		3	0.855	1.814	0.852	4	4	4	15
		4	0.849	1.834	0.849	3	3	3	6
		5	0.848	1.864	0.845	2	2	2	12
ICA-ANN	Training	1	0.873	1.592	0.873	4	4	4	12
		2	0.852	1.723	0.852	2	2	2	6
		3	0.876	1.574	0.876	5	5	5	15
		4	0.862	1.661	0.862	3	3	3	9
		5	0.839	1.796	0.839	1	1	1	3
	Testing	1	0.857	1.812	0.855	5	5	5	15
		2	0.852	1.816	0.852	3	3	3	9
		3	0.845	1.868	0.844	2	2	2	6
		4	0.853	1.814	0.853	4	4	4	12
		5	0.840	1.899	0.840	1	1	1	3

were employed to assess the developed models. As discussed in the previous sections, the performance indexes of the established models were sorted. According to Table 5, model no. 11 with 450 particles obtained the highest sorting value. As a result, 450 was determined to be the best N_{par} value.

Table 9 Results of total rank values of all stages of the developed final models

Method	Model no.	Total rank
MLR	1	1
MNR	1	1
ANN	1	20
	2	25
	3	9
	4	9
	5	27
GA-ANN	1	17
	2	18
	3	27
	4	13
	5	15
PSO-ANN	1	10
	2	30
	3	24
	4	13
	5	13
ICA-ANN	1	27
	2	15
	3	21
	4	21
	5	6

Value of the $N_{par\text{-}PSO}$

Different models with a fixed number of generations of 1000 and N_{par} in the range of 25–600 were developed to choose the optimum $N_{par\text{-}PSO}$. Figure 11 shows that the values of the RMSE do not change after the $N_{par\text{-}PSO}$ value of 800. Therefore, the optimum $N_{par\text{-}PSO}$ was set to 800 in this study.

Network modeling

Similarly, the PSO-ANN model was developed with ANN architecture of 6-15-1 and the obtained optimum parameters of PSO and was also trained five times. The performance index values of the final model are recorded in Table 8. The developed PSO-ANN model will be evaluated further in the "Results and discussion" section.

ICA-ANN models

The hybrid ICA-ANN model was also established to predict RQS. The hybrid ICA-ANN algorithm flowchart is shown in Fig. 12. The establishment process of the hybrid PSO-ANN prediction model will be discussed in the following sections.

ICA parameters

The main parameters of the ICA are the number of countries (N_{cou}), number of imperialists (N_{imp}), number of decades (N_{dec}), β (number greater than 1), θ (random number), and ξ (positive number less than 1). As previously mentioned, before establishing the hybrid model, the parameters β, θ, and ξ were selected as 1.5, $\pi/4$, and 0.2, respectively, according to the recommendations in the literature (Ahmadi et al. 2013; Marto et al. 2014). The remaining parameters of the N_{cou}, the N_{imp}, and the N_{dec} are determined in the following sections.

Value of N_{cou}

To select the optimal N_{cou}, different ICA-ANN models were developed with a range of N_{cou} from 50 to 600, as presented in Table 6. The ANN architecture of 6-15-1 and maximum decade of 100 were employed. Table 6 records the ranking results of the prediction performance indexes of the established prediction models. The results show that model no. 10, which represents 450 countries, has the largest ranking value. Thus, 450 was selected as the best N_{cou} value.

Value of N_{imp}

In this section, different ICA-ANN models were constructed with N_{imp} ranging from 50 to 200 and N_{cou} of 450. Table 7

Table 10 Results of the best performance indices of the developed final models

Method	No.	Training			Testing			Weight
		R^2	RMSE	VAF	R^2	RMSE	VAF	R^2 of testing
MLR	1	0.543	3.024	0.543	0.621	2.964	0.615	0.133
MNR	1	0.583	2.889	0.583	0.659	2.800	0.654	0.141
ANN	5	0.836	1.814	0.835	0.833	1.945	0.833	0.178
GA-ANN	3	0.833	1.828	0.833	0.840	1.905	0.839	0.180
PSO-ANN	2	0.875	1.584	0.875	0.862	1.782	0.861	0.185
ICA-ANN	1	0.873	1.592	0.873	0.857	1.812	0.855	0.183

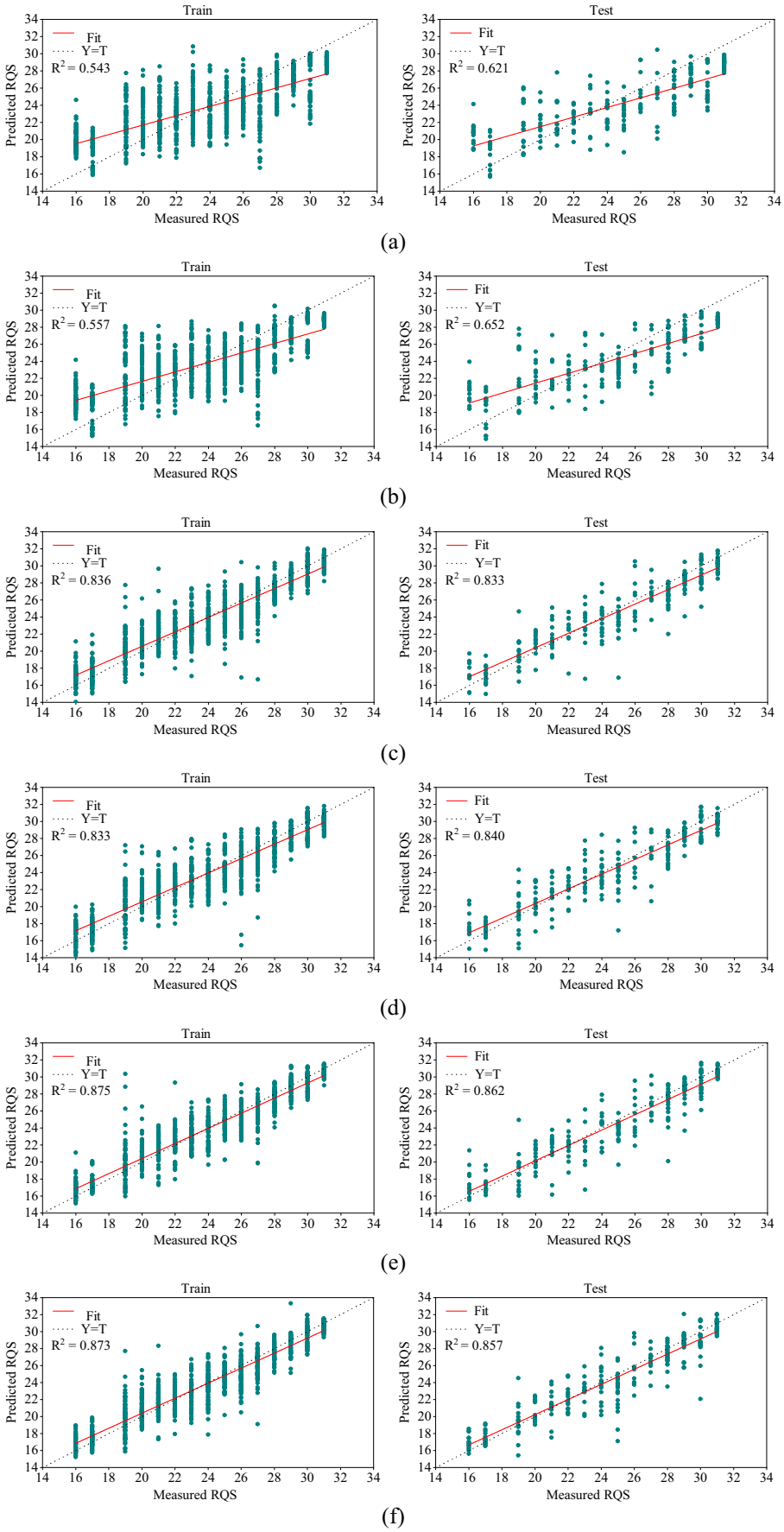

Fig. 14 The coefficient of determination of measured and predicted RQS values of five developed final models for training and testing datasets. **a** MLR. **b** MNR. **c** ANN. **d** The GA-ANN. **e** PSO-ANN. **f** ICA-ANN

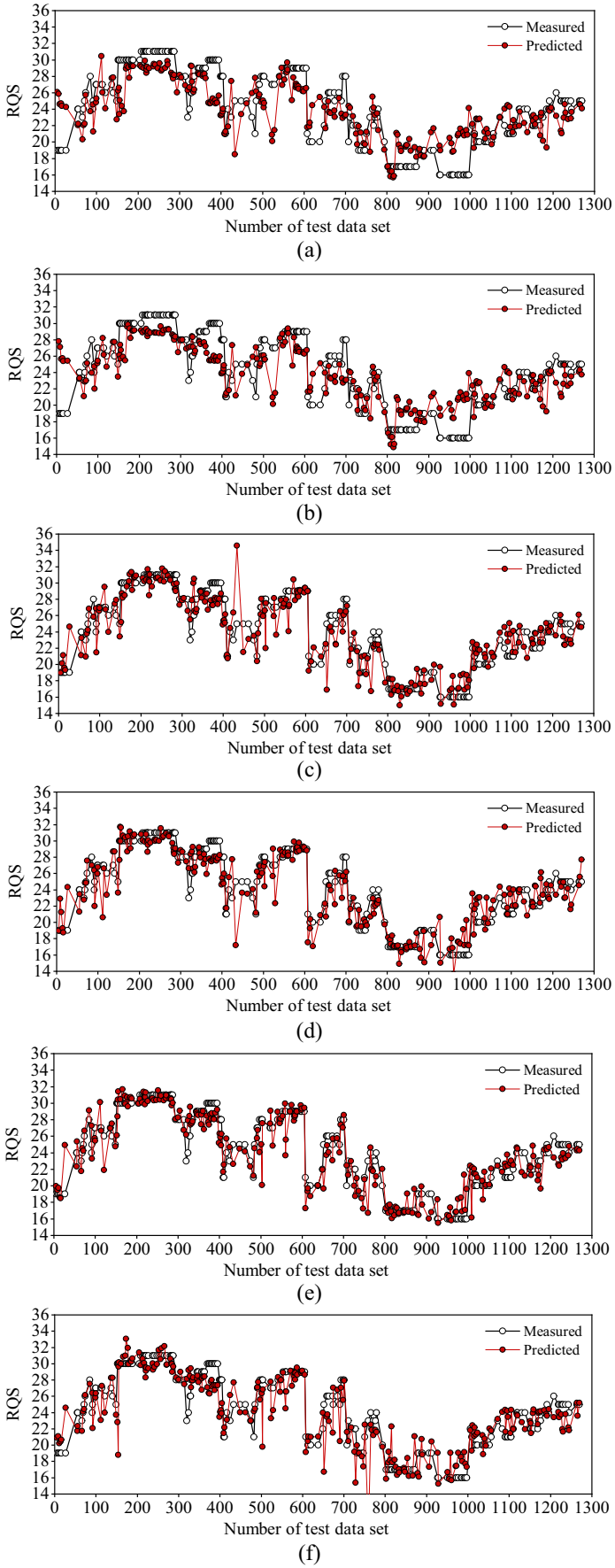

Fig. 15 Comparison of measured and predicted RQS values of five developed final models for training and testing datasets. **a** MLR. **b** MNR. **c** ANN. **d** The GA-ANN. **e** PSO-ANN. **f** ICA-ANN

shows that the no. 5 model representing $N_{imp} = 90$ has the highest sorting value. Therefore, 90 was set as the best N_{imp} value.

Value of the N_{dec}

As shown in Fig. 13, different models were developed to determine the best N_{dec} value with the fixed N_{dec} values of 1000 and the N_{cou} values between 50 and 600. The results show that the RMSE values of all models do not continue to decline after $N_{dec} = 800$. Therefore, 800 was determined as the best N_{dec} value of ICA-ANN prediction model.

Network modeling

As before with the developments of the GA-ANN and PSO-ANN models, the final ICA-ANN model was developed with the ANN architecture of 6-15-1 and determined optimal ICA parameters. The final ICA-ANN model was also trained five times. The performance index results of development models are shown in Table 8. All final prediction models established above will be discussed in next section.

Results and discussion

In this section, the final model previously developed will be compared to select the model with the highest predictive performance. In the last stage of the developing models, except MLR and MNR models, other models were trained five times to predict the RQS. The indices of R^2, RMSE, and VAF are utilized to assess the performance of these developed models.

Table 8 displays the obtained results of the developed models. Determining the optimal model is not easy because the results are similar. The method of ranking, as previously mentioned, was employed to select the optimal model in the same way. The total rank of all developed models is indicated in Table 9. The results show that ANN model no. 5, GA-ANN model no. 3, PSO-ANN model no. 2, and ICA-ANN model no. 1 have a total rank of 27, 27, 30, and 27, respectively, which indicates the optimal performance. For a certain training dataset, note that only one prediction formula can be fitted using the MLR method. Therefore, only one prediction model of the MLR was developed in this study.

Table 10 shows the best performance index results of the 6 final prediction models of MLR, MNR, GA-ANN, PSO-ANN, and ICA-ANN. The results revealed that the performance level of the regression models can be increased from approximately 0.60 (for MLR and MNR models) to approximately 0.83 (for ANN models) based on R^2 by developing the ANN model. The performance level of the ANN model can be increased based on R^2 by developing a hybrid model, i.e., PSO-ANN and ICA-ANN from approximately 0.83 (for ANN models) to approximately 0.86 (for PSO-ANN and ICA-ANN models). The measured and predicted RQS values of RQS obtained by the five optimal models are shown in Fig. 14. The comparison between measured RQS and predicted RQS using all five models with testing datasets are shown in Fig. 15. In addition, the weight of prediction effect of each model (Table 10) is obtained by calculating the proportion of R^2 value obtained by each model at the test stage in the total R^2 value of all models. It should be noted that the test stage is an important part of the evaluation of the prediction performance, and it should be emphasized that the test stage is an important part of the evaluation of the prediction effect and the change trend of the three evaluation indexes (R^2, RMSE, and VAF) is basically the same. Therefore, only the R^2 value of the test stage is considered when calculating the weight value of each model. Table 10 shows that MLR, MNR, ANN, GA-ANN, PSO-ANN, and ICA-ANN obtain weight values of 0.133, 0.141, 0.178, 0.180, 0.185, and 0.183 respectively. The results reveal that the hybrid models of PSO-ANN and ICA-ANN are better than the MLR, MNR, ANN, and GA-ANN models. When both the training dataset and the testing dataset are considered, R^2 values of 0.875 and 0.862 and R^2 values of 0.873 and 0.857 for the PSO-ANN technique and ICA-ANN technique, respectively, indicate that the PSO-ANN model has slightly higher performance compared with other models.

The comparison results of learning rates of ANN, GA-ANN, PSO-ANN, and ICA-ANN algorithms were shown in Fig. 16. ANN obtains the lowest RMSE value of 0.292 when epochs are about 160 steps. However, GA-ANN, PSO-ANN, and ICA-ANN got the lowest RMSE values when epochs are 80 steps, which are 0.212, 0.193, and 0.201, respectively. The results show that GA, PSO, and ICA can improve the learning rate of ANN and get better training effect.

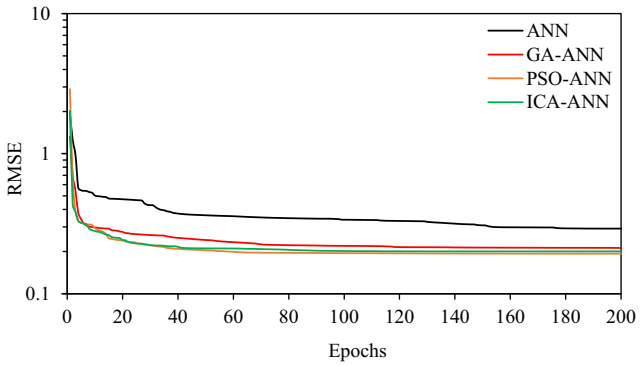

Fig. 16 Comparison of learning rates of ANN, GA-ANN, PSO-ANN, and ICA-ANN algorithms at the training stage

Table 11 Predicted large error values (top ten) of testing stages of the developed final models

Method	Testing dataset no.	Measured RQS	Predicted RQS	Error	Tunnel face no.
MLR	997	16	24.14	8.14	
	5	19	26.06	7.06	
	524	27	20.10	6.90	
	9	19	25.88	6.88	
	482	21	27.81	6.81	
	155	30	23.38	6.62	4
	433	25	18.50	6.50	1
	166	30	23.74	6.26	
	523	27	20.87	6.13	
	15	19	24.72	5.72	
MNR	5	19	27.88	8.88	
	9	19	27.14	8.14	
	524	27	19.91	7.09	
	997	16	22.81	6.81	
	523	27	20.25	6.75	
	11	19	25.73	6.73	
	27	19	25.41	6.41	2
	15	19	25.36	6.36	
	529	27	20.84	6.16	
ANN	433	25	34.57	9.57	1
	652	25	16.88	8.12	3
	759	23	16.73	6.27	
	503	28	22.01	5.99	5
	27	19	24.64	5.64	2
	559	29	24.06	4.94	
	152	30	25.20	4.80	4
	728	22	17.35	4.65	
	329	26	30.51	4.51	
	1095	21	25.08	4.08	
GA-ANN	433	25	17.18	7.82	1
	112	27	20.62	6.38	
	27	19	24.32	5.32	2
	425	23	27.73	4.73	
	927	16	20.67	4.67	
	529	27	22.34	4.66	
	324	24	28.41	4.41	6
	652	25	20.68	4.32	3
	991	16	20.27	4.27	
	890	19	15.08	3.92	
PSO-ANN	503	28	20.11	7.89	5
	759	23	16.74	6.26	
	27	19	24.92	5.92	2
	991	16	21.35	5.35	
	652	25	19.66	5.34	3
	560	29	23.69	5.31	
	1009	21	16.16	4.84	
	121	26	21.90	4.10	
	497	28	24.05	3.95	
	324	24	27.91	3.91	6
ICA-ANN	152	30	22.06	7.94	4
	433	25	17.10	7.90	1
	652	25	18.44	6.56	3
	27	19	24.52	5.52	2
	503	28	23.52	4.48	5
	1219	25	20.57	4.43	
	324	24	28.08	4.08	6
	154	30	25.96	4.04	4
	1221	25	21.02	3.98	
	779	24	20.16	3.84	

Furthermore, a statistical analysis of tunnel faces with large prediction error was carried out to reveal the reasons for low prediction performance, as shown in Table 11. Measured and predicted RQS, prediction error, and the number of corresponding testing datasets in the top 10 with large prediction error of the five final optimal models are recorded in this table. Tunnel faces 1–6 of testing datasets 433, 27, 652, 152(155), 503, and 324 achieved low prediction performance in at least three prediction models. The detailed geological description site photos of tunnel faces 1–6 are shown in Fig. 17. As displayed in Fig. 17, these tunnel faces have the geological characteristics of relatively developed cracks and ground water heavy deterioration. For example, many large cracks exist in the tunnel faces 1–6; large sheeting zones exist in tunnel faces 1, 4, 5, and 6; and water inrush deterioration is relatively serious in tunnel faces 3–5. The findings conclude that the MWD data of a single borehole cannot sufficiently characterize the complex rock mass quality. Therefore, when the complex rock mass is continuously exposed in the tunnel excavation, the application of more than one borehole for advance detection is suggested to improve the prediction accuracy.

Finally, it should be noted that the best prediction model is determined as PSO-ANN hybrid model, and the corresponding ANN structure is 6-15-1. In this structure, all six variables were taken as input variables. According to the results of relative influence of each input variable on RQS in the "Dataset collection and analysis" section, the weight values of 0.26, 0.01, 0.11, 0.36, 0.05, and 0.20 were obtained for PR, HP, RP, FP, HF, and SE respectively. In practical application, the weight values can be used to determine the final required input variables.

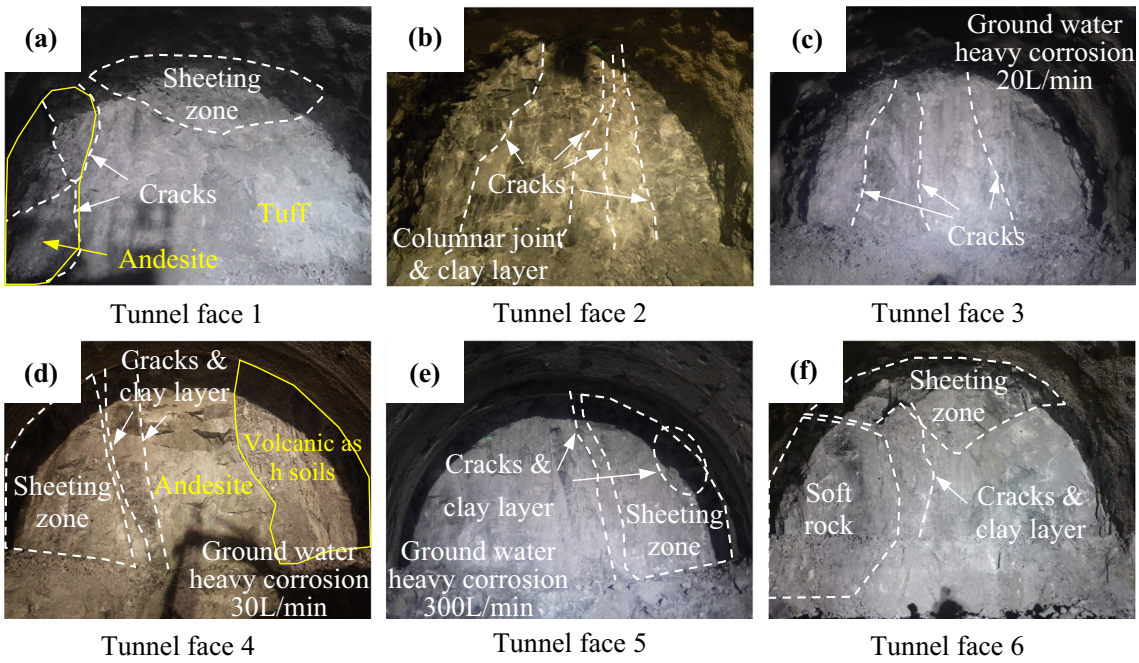

Fig. 17 Tunnel faces with low prediction performance. **a** Tunnel face 1 (chainage of 58 K533.9). **b** Tunnel face 2 (chainage of 57K990.0). **c** Tunnel face 3 (chainage of 59 K142.4). **d** Tunnel face 4 (chainage of 58K227.0). **e** Tunnel face 5 (chainage of 58 K759.5). **f** Tunnel face 6 (chainage of 58K311.9)

Conclusion

The accurate/objective prediction of the rock mass quality score (RQS) utilizing measure-while-drilling (MWD) data is one of the greatest challenges in tunneling operations. An advantage of artificial neural network (ANN) methods is that they can address complex multivariate nonlinear mapping problems. However, it is required to overcome the shortcomings of slow training speed and minimum layout through optimization ANN, so as to produce more reliable results in the prediction of RQS. Therefore, three optimization algorithms of the genetic algorithm (GA), particle swarm optimization (PSO), and imperialist competition algorithm (ICA) were employed to develop hybrid models of GA-ANN, PSO-ANN, and ICA-ANN to predict the RQS value. For this purpose, 1270 datasets, including six measure-while-drilling parameters of penetration rate (PR), hammer pressure (HP), rotation pressure (RP), feed pressure (FP), hammer frequency (HF), and specific energy (SE), were acquired from the new Nagasaki tunnel (east) of the West Kyushu Line high-speed railway in Japan and considered input parameters, while their corresponding RQS were considered output parameters. To compare the performance of the hybrid models, MLR and ANN models were also developed to predict the RQS.

Three performance indexes R^2, RMSE, and VAF are used to compare the developed prediction model. The results show that the developed PSO-ANN and ICA-ANN models have higher accuracy and efficiency than other models. However, among the two hybrid models, the PSO-ANN hybrid model has slightly higher performance in predicting RQS. The results of $R^2 = 0.875$ and 0.862, RMSE = 1.584 and 1.782, and VAF = 0.875 and 0.861 for the training dataset and testing dataset, and the results of $R^2 = 0.873$ and 0.857, RMSE = 1.592 and 1.812, and VAF = 0.873 and 0.855 for the training dataset and testing dataset were obtained for the PSO-ANN model and ICA-ANN model, respectively.

Note that the models established in this paper are specific to the West Kyushu Line of the high-speed railway region, and the parameters of the final prediction model need to be modified according to their conditions for other regions and other tunnel construction methods. Based on the hybrid ANN algorithm proposed in this paper, the research on the influence of different combinations of MWD parameters on prediction performance needs to be further explored.

Funding The authors gratefully acknowledge the support from the Konoike Construction Japan in field data collection and data analysis.

Compliance with ethical standards

Conflict of interest The authors declare that they have no conflict of interest.

References

Ahmadi MA, Ebadi M, Shokrollahi A, Majidi SMJ (2013) Evolving artificial neural network and imperialist competitive algorithm for prediction oil flow rate of the reservoir . Appl Soft Comput 13: 1085–1098. https://doi.org/10.1016/j.asoc.2012.10.009

Akagi W, Sano A, Shinji M, Nishi T, Nakagawa K (2001) A new rock mass classification method at tunnel face for tunnel support system. Doboku Gakkai Ronbunshu 2001:121–134

Aoki K, Shirasagi S, Yamamoto T, Inou M, Nishioka K (1999) Examination of the application of drill logging to predict ahead of the tunnel face. In: Proceedings of the 54th Annual Conference of the Japan Society of Civil Engineers, Tokyo, Japan, September 1999, pp 412–413

Armaghani DJ, Hasanipanah M, Mahdiyar A, Abd Majid MZ, Bakhshandeh Amnieh H, Tahir MMD (2018) Airblast prediction through a hybrid genetic algorithm-ANN model. Neural Comput Appl 29:619–629. https://doi.org/10.1007/s00521-016-2598-8

Armaghani DJ, Koopialipoor M, Marto A, Yagiz S (2019) Application of several optimization techniques for estimating TBM advance rate in granitic rocks. J Rock Mech Geotech Eng 11:779–789. https://doi.org/10.1016/j.jrmge.2019.01.002

Atashpaz-Gargari E, Lucas C (2007) Imperialist competitive algorithm: An algorithm for optimization inspired by imperialistic competition. In: 2007 IEEE Congress on Evolutionary Computation, 25–28 Sept 2007, pp 4661–4667. https://doi.org/10.1109/CEC.2007.4425083

Back AD, Chen T (2002) Universal approximation of multiple nonlinear operators by neural networks. Neural Comput 14:2561–2566

Barton N, Lien R, Lunde J (1974) Engineering classification of rock masses for the design of tunnel support. Rock Mech 6:189–236. https://doi.org/10.1007/bf01239496

Bieniawski Z (1973) Engineering classification of jointed rock masses. Civil Engineer in South Africa 15

Clerc M, Kennedy J (2002) The particle swarm-explosion, stability, and convergence in a multidimensional complex space. IEEE Trans Evol Comput 6:58–73

Deere DU (1964) Technical description of rock cores for engineering purpose. Rock Mechanics and Engineering Geology 1:17–22

Dybowski R, Gant V, Weller P, Chang R (1996) Prediction of outcome in critically ill patients using artificial neural network synthesised by genetic algorithm. The Lancet 347:1146–1150. https://doi.org/10.1016/S0140-6736(96)90609-1

Erharter GH, Marcher T, Reinhold C (2019) Artificial neural network based online rockmass behavior classification of TBM data. In: Information technology in geo-engineering. Springer International Publishing, Cham, pp 178–188

Gandomi AH, Yun GJ, Yang X-S, Talatahari S (2013) Chaos-enhanced accelerated particle swarm optimization. Commun Nonlinear Sci Numer Simul 18:327–340. https://doi.org/10.1016/j.cnsns.2012.07.017

Gao D (1998) On structures of supervised linear basis function feedforward three-layered neural networks Chinese Journal of Computers 1

Gazafroudi AS, Bigdeli N, Ramandi MY, Afshar K (2014) A hybrid model for wind power prediction composed of ANN and imperialist competitive algorithm (ICA). In: 2014 22nd Iranian Conference on Electrical Engineering (ICEE), 20–22 May 2014, pp 562–567. https://doi.org/10.1109/IranianCEE.2014.6999606

Han W, Li G, Sun Z, Luan H, Liu C, Wu X (2020) Numerical investigation of a foundation pit supported by a composite soil nailing structure. Symmetry 12:252

Hasanipanah M, Jahed Armaghani D, Bakhshandeh Amnieh H, Majid MZA, Tahir MMD (2017) Application of PSO to develop a powerful equation for prediction of flyrock due to blasting. Neural Comput Appl 28:1043–1050. https://doi.org/10.1007/s00521-016-2434-1

Hoballah A, Erlich I (2009) PSO-ANN approach for transient stability constrained economic power generation. In: 2009 IEEE Bucharest PowerTech, 28 June–2 July 2009, pp 1–6. https://doi.org/10.1109/PTC.2009.5281926

Hoek E, Brown ET (1997) Practical estimates of rock mass strength. Int J Rock Mech Min Sci 34:1165–1186. https://doi.org/10.1016/S1365-1609(97)80069-X

Holland JH (1992) Adaptation in natural and artificial systems: an introductory analysis with applications to biology, control, and artificial intelligence. MIT Press

Hornik K (1991) Approximation capabilities of multilayer feedforward networks. Neural Networks 4:251–257. https://doi.org/10.1016/0893-6080(91)90009-T

Hussain S, Mohammad N, Khan M, Rehman ZU, Tahir M (2016) Comparative analysis of rock mass rating prediction using different inductive modeling techniques. International Journal of Mining Engineering Mineral Processing 5:9–15

Kanellopoulos I, Wilkinson GG (1997) Strategies and best practice for neural network image classification. Int J Remote Sens 18:711–725

Karlaftis A (2018) Classifying rock masses using artificial neural networks. In: Geoecology and computers. Routledge, pp 279–284

Kayabasi A (2012) Prediction of pressuremeter modulus and limit pressure of clayey soils by simple and non-linear multiple regression techniques: a case study from Mersin, Turkey. Environ Earth Sci 66:2171–2183

Kennedy J, Eberhart R (1995) Particle swarm optimization (PSO). In: Proc. IEEE International Conference on Neural Networks, Perth, pp 1942–1948

Kennedy J, Eberhart RC (1997) A discrete binary version of the particle swarm algorithm. In: 1997 IEEE International Conference on Systems, Man, and Cybernetics. Computational Cybernetics and Simulation, 12–15 Oct 1997, vol 4105, pp 4104-4108. https://doi.org/10.1109/ICSMC.1997.637339

Khandelwal M, Mahdiyar A, Armaghani DJ, Singh TN, Fahimifar A, Faradonbeh RS (2017) An expert system based on hybrid ICA-ANN technique to estimate macerals contents of Indian coals. Environ Earth Sci 76:399. https://doi.org/10.1007/s12665-017-6726-2

Knofczynski GT, Mundfrom D (2008) Sample sizes when using multiple linear regression for prediction. Educ Psychol Meas 68:431–442

Lear WE, Dareing DW (1990) Effect of drillstring vibrations on MWD pressure pulse signals. J Energy Res Technol 112:84

Leung R, Scheding S (2015) Automated coal seam detection using a modulated specific energy measure in a monitor-while-drilling context. Int J Rock Mech Min Sci 75:196–209. https://doi.org/10.1016/j.ijrmms.2014.10.012

Li SC, Wu J, Xu ZH, Li LP (2017) Unascertained measure model of water and mud inrush risk evaluation in karst tunnels and its engineering application. KSCE J Civ Eng 21:1170–1182. https://doi.org/10.1007/s12205-016-1569-z

Liu J, Luan H, Zhang Y, Sakaguchi O, Jiang Y (2020) Prediction of unconfined compressive strength ahead of tunnel face using measurement-while-drilling data based on hybrid genetic algorithm. Geotech Eng 22. https://doi.org/10.12989/gae.2020.22.1.000

Looney CG (1996) Advances in feedforward neural networks: demystifying knowledge acquiring black boxes. IEEE Transactions on Knowledge Data Engineering, pp 211–226

Lowson A, Bieniawski Z (2013) Critical assessment of RMR based tunnel design practices: a practical engineer's approach. In: Proceedings of the SME, Rapid Excavation and Tunnelling Conference, Washington, DC, pp 23–26

Lu J, Liu X (2009) Construction techniques for water and sand gushing section in Xiushan Tunnel on Yuxi-Mengzi railway. Tunnel Construction 3

Marto A, Hajihassani M, Jahed Armaghani D, Tonnizam Mohamad E, Makhtar AM (2014) A novel approach for blast-induced flyrock prediction based on imperialist competitive algorithm and artificial neural network. The Scientific World Journal 2014

Masahiro N, Koji M, Hiroshi Y, Takuro N, Kazuo N, Koji N (1999) A new proposal of evaluation system for tunnel face based on the analysis of the observation records. Journal of Japan Society of Civil Engineers 623:131–141

McCulloch WS, Pitts W (1943) A logical calculus of the ideas immanent in nervous activity. The Bulletin of Mathematical Biophysics 5: 115–133. https://doi.org/10.1007/bf02478259

Moayedi H, Jahed Armaghani D (2018) Optimizing an ANN model with ICA for estimating bearing capacity of driven pile in cohesionless soil. Eng Comput 34:347–356. https://doi.org/10.1007/s00366-017-0545-7

Moayedi H, Mehrabi M, Mosallanezhad M, Rashid ASA, Pradhan B (2019) Modification of landslide susceptibility mapping using optimized PSO-ANN technique. Eng Comput 35:967–984. https://doi.org/10.1007/s00366-018-0644-0

Mohamad ET, Hajihassani M, Armaghani DJ, Marto A (2012) Simulation of blasting-induced air overpressure by means of artificial neural networks. Int Rev Modell Simulations 5:2501–2506

Momeni E, Nazir R, Jahed Armaghani D, Maizir H (2014) Prediction of pile bearing capacity using a hybrid genetic algorithm-based ANN. Measurement 57:122–131. https://doi.org/10.1016/j.measurement.2014.08.007

Momeni E, Nazir R, Armaghani DJ, Maizir H (2015) Application of Artificial Neural Network for predicting shaft and tip resistances of concrete piles. Earth Sci Res J 19:85–93

Monjezi M, Ghafurikalajahi M, Bahrami A (2011) Prediction of blast-induced ground vibration using artificial neural networks. Tunn Undergr Space Technol 26:46–50. https://doi.org/10.1016/j.tust.2010.05.002

Monjezi M, Hasanipanah M, Khandelwal M (2013) Evaluation and prediction of blast-induced ground vibration at Shur River Dam, Iran, by artificial neural network. Neural Computing Applications and Applied Mathematics 22:1637–1643

Nasseri M, Asghari K, Abedini MJ (2008) Optimized scenario for rainfall forecasting using genetic algorithm coupled with artificial neural network. Expert Syst Appl 35:1415–1421. https://doi.org/10.1016/j.eswa.2007.08.033

Navarro J, Sanchidrián J, Segarra P, Castedo R, Costamagna E, López L (2018) Detection of potential overbreak zones in tunnel blasting from MWD data. Tunn Undergr Space Technol 82:504–516. https://doi.org/10.1016/j.tust.2018.08.060

Nelson MM, Illingworth WT (1991) A practical guide to neural nets

Nilsen B (2015) Main challenges for deep subsea tunnels based on norwegian experience. J of Korean Tunn Undergr Sp Assoc 17:563–573. https://doi.org/10.9711/KTAJ.2015.17.5.563

Nouiri M, Bekrar A, Jemai A, Niar S, Ammari AC (2018) An effective and distributed particle swarm optimization algorithm for flexible job-shop scheduling problem. J Intell Manuf 29:603–615. https://doi.org/10.1007/s10845-015-1039-3

Palmstrom A (2005) Measurements of and correlations between block size and rock quality designation (RQD). Tunn Undergr Space Technol 20:362–377. https://doi.org/10.1016/j.tust.2005.01.005

Rahmati A, Faramarzi L, Sanei M (2014) Development of a new method for RMR and Q classification method to optimize support system in tunneling. Frontiers of Structural Civil Engineering 8:448–455. https://doi.org/10.1007/s11709-014-0262-x

Rehman H, Naji AM, Kim J-J, Yoo H-K (2018) Empirical evaluation of rock mass rating and tunneling quality index system for tunnel support design. Appl Sci 8:782

Rosenblatt F (1958) The perceptron: a probabilistic model for information storage and organization in the brain. Psychol Rev 65:386

Shi Y, Eberhart RC (1998) Parameter selection in particle swarm optimization. In: Evolutionary Programming VII. Springer, Berlin Heidelberg, pp 591–600

Shin HS, Han KC, Sunwoo C, Choi SO, Choi YK (1999) Collapse of a tunnel in weak rock and the optimal design of the support system. Paper presented at the 9th ISRM Congress, Paris, 1999

Sousa LR, Miranda T, Roggenthen W, Sousa RL (2012) Models for geomechanical characterization of the rock mass formations at DUSEL using data mining techniques. Paper presented at the 46th U.S. Rock Mechanics/Geomechanics Symposium, Chicago, Illinois, 2012

Swingler K (1996) Applying neural networks: a practical guide. Morgan Kaufmann

Vasumathi B, Moorthi S (2012) Implementation of hybrid ANN–PSO algorithm on FPGA for harmonic estimation. Eng Appl Artif Intell 25:476–483. https://doi.org/10.1016/j.engappai.2011.12.005

Wang C, Jiang Y, Liu R, Wang C, Zhang Z, Sugimoto S (2020a) Experimental study of the nonlinear flow characteristics of fluid in 3D rough-walled fractures during shear process. Rock Mech Rock Eng 53:2581–2604. https://doi.org/10.1007/s00603-020-02068-5

Wang X, Yuan W, Yan Y, Zhang X (2020b) Scale effect of mechanical properties of jointed rock mass: A numerical study based on particle flow code. Geotech Eng 21:259–268

Xu J, Wang J, Ma Y (2007) Rock mass quality assessment based on BP artificial neural network (ANN). A case study of borehole BS03 in Jiujing segment of Beishan, Gansu. Uranium Geology 23:243, 249–256

Yang X-S (2010) Engineering optimization: an introduction with metaheuristic applications. John Wiley & Sons

Yilmaz I (2009) A new testing method for indirect determination of the unconfined compressive strength of rocks. Int J Rock Mech Min Sci 46:1349–1357

Yue ZQ, Lee CF, Law KT, Tham LG (2004) Automatic monitoring of rotary-percussive drilling for ground characterization—illustrated by a case example in Hong Kong. Int J Rock Mech Min Sci 41: 573–612. https://doi.org/10.1016/j.ijrmms.2003.12.151

Yuji W, Tatsuo K, Masaki K, Kenichi H (2006) Solution with modified perceptron to tunnel cutting face evaluation problems. Geoinformatics 17:61–70

Zhou H, Hatherly P, Ramos F, Nettleton E (2011) An adaptive data driven model for characterizing rock properties from drilling data. In: 2011 IEEE International Conference on Robotics and Automation, Shanghai, China, May 2011. IEEE, pp 1909–1915

Zolfaghari A, Sohrabi Bidar A, Maleki Javan MR, Haftani M, Mehinrad A (2015) Evaluation of rock mass improvement due to cement grouting by Q-system at Bakhtiary dam site. Int J Rock Mech Min Sci 74:38–44. https://doi.org/10.1016/j.ijrmms.2014.12.004

Zorlu K, Gokceoglu C, Ocakoglu F, Nefeslioglu HA, Acikalin S (2008) Prediction of uniaxial compressive strength of sandstones using petrography-based models. Eng Geol 96:141–158. https://doi.org/10.1016/j.enggeo.2007.10.009